C.P. No. 1049

C.P. No. 1049

MINISTRY OF TECHNOLOGY

AERONAUTICAL RESEARCH COUNCIL

CURRENT PAPERS

Short-Cowl Front-Fan Turbojets; Friction Drag and Wall-Jet Effects on Cylindrical Afterbodies

by

J. E. Green.

Aerodynamics Dept., R.A.E., Bedford

LONDON HER MAJESTY'S STATIONERY OFFICE

1969

PRICE 7s 6d NET

U.D.C. 621.438 + 629.13.038.5 : 533.6.013.124 : 629.13.012.122 :
533.697.4 : 533.695.27 : 533.696.8

C.P. No.1049*
June 1967

SHORT-COWL FRONT-FAN TURBOJETS; FRICTION DRAG AND WALL-JET EFFECTS ON CYLINDRICAL AFTERBODIES

by

J. E. Green

SUMMARY

An approximate analysis is given of a turbulent wall-jet beneath a stream moving at constant velocity. The results of this analysis are used to predict the drag of a cylindrical afterbody immersed in the jet from a front fan with short cowl at subsonic flight speeds. Graphs are presented which allow rapid evaluation of afterbody drag for a range of jet pressure ratios and nacelle geometries.

---

*Replaces R.A.E. Technical Report 67144 - A.R.C. 29545.

CONTENTS

1 INTRODUCTION

The advent of turbofan engines with short front cowls has seen an increase in the difficulty of predicting nacelle drag. The nacelle afterbody, which produces a considerable proportion of the total nacelle drag, is now isolated from the free stream by the annular jet from the fan. The result is a high skin-friction drag on the afterbody due to the high velocity of the fan jet, and a flow field which in the general case is difficult to analyse with confidence.

This Paper concentrates on a single aspect of the problem: the possibility that the decay of jet velocity due to mixing between jet and free stream might lead, over the rear of the afterbody, to some alleviation of this high friction drag. For a given nacelle configuration afterbody drag is determined and presented as a fraction of what it would be if there were no mixing between jet and free stream. The governing parameters are the ratio of afterbody length to initial depth of jet and the velocity ratio between jet and free stream.

The treatment is confined to fully expanded jets flowing at constant pressure over cylindrical afterbodies, and is derived from an analysis of the flow of a turbulent wall-jet into still air. Because drag reductions in most practical cases turn out to be small or non-existent, the approximate nature of some parts of the analysis is thought not to be an important limitation.

2 OUTLINE OF TREATMENT

When fully expanded, the outlet stream from a front fan is ideally a uniform jet with the same static pressure and temperature* as the external stream, but with a higher velocity. The flow field produced by the interaction between this jet, the wall and the external stream is illustrated in Fig.1.

For a distance x_c downstream of its exit plane the jet retains an irrotational core of velocity u_j. The boundary layer on the wall and the shear layer between jet and free stream eat into this core until at x_c the edges of the two layers meet. Thereafter the maximum velocity of the jet diminishes with distance and the flow passes through a short transitional region to emerge with the properties of a fully developed wall-jet. This latter type of flow then persists for some appreciable distance downstream.

---

*In section 4.2 we note that in practice, because of losses in the fan, there is not exact equality of temperatures.

Eventually, at large distances, the growing boundary layer on the wall submerges the jet and finally, at very large distances, all influence of the jet on the character of the flow vanishes. In the present context there is no practical interest in these later stages of the flow, and so the treatment is not taken beyond the fully developed wall-jet region.

We begin by developing a treatment of the drag which a two-dimensional incompressible jet flowing into still air exerts on its adjacent wall. This treatment is then extended to apply to jets beneath streams moving with constant velocity. Finally, the modifications needed to make it applicable to compressible flows around cylindrical afterbodies are discussed, and the results are presented in a form convenient for making drag estimates.

It has to be assumed at the outset that vorticity shed from the fan will have no significant effect on the mixing between jet and free stream, or on the wall shear stress. We can then treat the jet flow as initially irrotational, and so make use of empirical relations obtained in other studies of this type of flow. For simplicity it is assumed that the initial boundary layers at the jet exit plane are negligible, and the region of transition between the partly irrotational jet and the fully developed wall-jet is also neglected. Other assumptions needed are discussed as they arise in the text.

3 WALL-JET DRAG IN TWO-DIMENSIONAL INCOMPRESSIBLE FLOW

3.1 Wall-jet in still air

Fig.2 shows typical profiles of mean velocity and shear stress measured by Bradshaw and Gee[1] in a fully developed turbulent wall-jet flowing into still air. Our present concern is the wall shear stress τ_w and its dependence on the other properties of the profile. We shall denote conditions at the velocity maximum by the subscript m, and call the region between the velocity maximum and the wall the "inner layer".

Bradshaw and Gee found that the friction coefficient $\tau_w/\frac{1}{2}\rho u_m^2$ and an inner layer Reynolds number $\frac{u_m y_m}{\nu}$ satisfied a relation of the form

$$\frac{\tau_w}{\frac{1}{2}\rho u_m^2} = A\left(\frac{u_m y_m}{\nu}\right)^{-\alpha} . \qquad (1)$$

They noted that the constants A and α which gave the best fit to their measurements differed from those appropriate to the boundary layer on a flat plate. Their observed Reynolds number dependency broadly agrees with the results of Sigalla[2] (though he found values of A and α from conventional boundary-layer relations to be adequate) and those of R.P. Patel[3].

We may note in passing that the prediction by Schwarz and Cosart[4], that $\tau_w/\frac{1}{2}\rho u_m^2$ is constant in a given wall-jet flow, is not borne out by these experimental results. However, Schwarz and Cosart made their prediction on the assumption that the flow was self-preserving. By revealing a streamwise variation in $\tau_w/\frac{1}{2}\rho u_m^2$, the experiments of Refs.1-3 imply that true self-preservation does not extend to the inner part of a wall-jet.

Accepting that equation (1) describes the dependency of τ_w on the Reynolds number of the inner layer, we now need to predict the streamwise development of this Reynolds number. To this end we shall treat the inner layer as a boundary layer, with displacement and momentum thicknesses defined as:

$$\left.\begin{aligned} \delta^* &= \int_0^{y_m} \left(1 - \frac{u}{u_m}\right) dy \\ \theta &= \int_0^{y_m} \frac{u}{u_m}\left(1 - \frac{u}{u_m}\right) dy \end{aligned}\right\} \quad . \tag{2}$$

The momentum integral equation for the region $0 < y < y_m$, derived in Appendix A, is:

$$\frac{d\theta}{dx} = \frac{\tau_w}{\rho u_m^2} - \frac{\tau_m}{\rho u_m^2} + \frac{1}{u_m}\frac{du_m}{dx}\left[y_m - \delta^* - 2\theta\right] \quad . \tag{3}$$

The second and third terms on the r.h.s. of this equation, though omitted in Lawrence's[5] treatment of nacelle drag, are both of the same order as the wall shear stress term. Furthermore, since $\partial u/\partial y$ is zero at y_m, the determination of τ_m appears difficult. (For one thing, eddy viscosity arguments are of no use.)

However, from the experimental shear stress distribution of Bradshaw and Gee (Fig.2), we see that shear stress variation over the inner region is closely linear. Thus it is a fairly good approximation to write

$$\tau_w - \tau_m = -y_m \left(\frac{\partial \tau}{\partial y}\right)_m \quad . \tag{4}$$

Also, the streamwise equation of motion

$$u \frac{\partial u}{\partial x} + v \frac{\partial u}{\partial y} = -\frac{1}{\rho} \frac{dp}{dx} + \frac{1}{\rho} \frac{\partial \tau}{\partial y}$$

reduces at y_m to

$$u_m \frac{du_m}{dx} = \frac{1}{\rho} \left(\frac{\partial \tau}{\partial y}\right)_m \quad . \tag{5}$$

Combining equations (3), (4) and (5) we obtain

$$\frac{d\theta}{dx} = -\frac{1}{u_m} \frac{du_m}{dx} (\delta^* + 2\theta)$$

or,

$$\frac{1}{\theta} \frac{d\theta}{dx} = -\frac{1}{u_m} \frac{du_m}{dx} (H + 2) \quad . \tag{6}$$

Since the streamwise variation of H $(= \delta^*/\theta)$ in the inner layer of wall-jet flow is small, $H + 2$ is effectively constant and equation (6) may be integrated to give

$$\frac{\theta_2}{\theta_1} = \left(\frac{u_{m_1}}{u_{m_2}}\right)^{H+2} \tag{7}$$

where subscripts 1 and 2 refer to two streamwise stations.

A further consequence of the almost constant shape of the inner velocity profile is that y_m/θ remains approximately constant and equation (1) may be written

$$\frac{\tau_w}{\frac{1}{2} \rho u_m^2} = B \left(\frac{u_m \theta}{\nu}\right)^{-\alpha} \quad . \tag{8}$$

Combining equations (7) and (8) we obtain

$$\frac{\tau_{w_2}}{\tau_{w_1}} = \left(\frac{u_{m_2}}{u_{m_1}}\right)^{\beta} , \qquad (9)$$

where

$$\beta = 2 + (H + 1)\alpha , \qquad (10)$$

and the drag of the wall may be obtained if the streamwise distribution of u_m is known.

In a later section a value of 2.36 is chosen for β. We may thus note that a fall in τ_w is due mostly to streamwise decay of ρu_m^2 and is only weakly affected by variation of $\frac{u_m \theta}{\nu}$. Hence the uncertainty involved in evaluating τ_m from equation (4) is not crucially important to the prediction of surface drag.

3.2 Extension to flow beneath an external stream

It is assumed at the outset that the analysis of the preceding section may be applied without change to wall-jets beneath moving streams.

In effect, this is largely the assumption that equation (4) still holds in this case. Clearly it fails in the limit where the velocities of jet and external stream are equal and du_m/dx is zero. Nevertheless, for the intermediate case where the free stream velocity and the excess velocity of the jet are of the same order, it is suggested that it provides an acceptable, simple approach to the unknown $\tau_m/\rho u_m^2$ in equation (3).

Given this assumption, and a value for the exponent β in equation (9), the problem is reduced to determining the streamwise distribution of u_m. For wall-jets at high Reynolds number beneath moving streams there is a scarcity of experimental data, and prediction of these flows necessitates an element of speculation.

Here the problem is approached by postulating that in the limit of very high Reynolds number the flow tends towards that on one side of the plane of symmetry of a free jet. In effect, we regard the wall-jet as a perturbation of this free jet flow. The boundary conditions $\tau = 0$, $u = u_{max}$ on the axis of the free jet are changed to $\tau = \tau_w$, $u = 0$ by the presence of the wall. The peak velocity now occurs some distance away from the axis and is less than the

peak velocity of the original jet. It is argued, however, that at high Reynolds number this distance becomes small and the difference between u_{max} and u_m vanishes.

For free jets, Reynolds number is generally discounted as a significant parameter. Dimensional analysis then suggests that a relation exists of the form

$$\frac{u_m}{u_e} = f\left(\frac{x'}{\lambda}\right) \tag{11}$$

where u_e is the velocity of the external stream, x' is distance from an effective origin, and

$$2\lambda = \text{excess momentum flux of jet} \times \frac{1}{\rho u_e^2}$$

$$= 2h \frac{u_j}{u_e}\left(\frac{u_j}{u_e} - 1\right) \tag{12}$$

here 2h is the width of the jet and u_j is its initial velocity.

The recent experimental results of Bradbury and Riley[6] have been used to define equation (11) for the range of u_m/u_e which is of interest here. Fig.3 shows these results. For the present purpose they have been fitted with the empirical relation*

$$\frac{u_m}{u_e} = 1 + 3.8\left(\frac{x'}{\lambda}\right)^{-0.555} . \tag{13}$$

It will be assumed that at high Reynolds numbers this expression provides a reasonably accurate description of the decay of peak velocity in the case of a wall-jet also**. From equations (7), (9) and (13) the important inner-layer parameters may now be evaluated through the region of fully-developed wall-jet flow. To complete the analysis, a treatment is needed of the region

---

* The exponent of distance in equation (13) is the same as that suggested by Schwarz and Cosart for the still-air wall-jet. This is fortuitous and probably not particularly significant.

**Because of wall friction, the excess momentum of the jet slowly decays with distance from the orifice. λ is evaluated from its initial value.

immediately downstream of the orifice where the jet retains an irrotational core.

3.3 The irrotational core

The flow field produced by a jet beneath a stream is illustrated in Fig.1. For a distance x_c downstream of its exit plane the jet retains a core of irrotational flow of velocity u_j. At x_c the outer edge of the wall boundary-layer meets the inner edge of the free shear-layer between jet and stream, and thereafter a wall-jet flow develops with its virtual origin a distance $x' - x$ upstream of the jet exit.

The transitional region immediately downstream of x_c, where $u_m < u_j$ but the wall-jet flow is not fully developed, will be neglected for the sake of simplicity. So too will the boundary layers on the nacelle and inside the nozzle upstream of the jet exit plane. Thus the wall boundary-layer and the free shear-layer are assumed to originate at the jet exit plane, and at their point of confluence x_c the flow is assumed to be that of a fully developed wall-jet.

The rate of encroachment of the shear-layer on the irrotational core of the jet, i.e. the rate at which it entrains high velocity fluid, is taken from a result derived in Ref.7 and elsewhere. Writing this as F (the shear layer spreads into the jet core at an angle $\tan^{-1}F$) we have, in the present notation

$$F = \frac{\pi}{96}\left(\frac{u_j - u_e}{u_j + u_e}\right)\left(\frac{3u_j + u_e}{u_j}\right) \quad . \tag{14}$$

The growth of the wall boundary-layer is non-linear and weakly dependent on Reynolds number. However, since the range of Reynolds numbers of practical interest is not large, the rate of growth of this layer is taken as a constant. For the turbulent boundary layer on a flat plate at a length Reynolds number of 10^7,

$$\left(\frac{\delta}{x}\right)_c \simeq 0.015 \quad . \tag{15}$$

(For a flat plate boundary layer $\delta/\theta \simeq 10$ - a one-seventh power law gives 7/72 - and $\theta/x \simeq 0.0015$ at $R_x = 10^7$.)

Then, since from Fig.1

$$h = \delta_c + Fx_c \quad , \tag{16}$$

we obtain from equations (14) and (15)

$$\frac{h}{x_c} = \frac{\pi}{96}\left(\frac{u_j - u_e}{u_j + u_e}\right)\left(\frac{3u_j + u_e}{u_j}\right) + 0.015 \quad . \tag{17}$$

Now, if the wall-jet is fully developed at x_c, we may write equation (13)

$$\frac{u_j}{u_e} = 1 + 5.8\left(\frac{x'_c}{\lambda}\right)^{-0.555} \tag{18}$$

where λ is given by equation (12).

Thus, given the ratio of jet and free stream velocities and the orifice height h, we can determine x_c from equation (17) and x'_c (and hence the virtual origin of the wall-jet flow) from equations (18) and (12). Finally, the streamwise distribution of u_m is obtained from equation (13).

3.4 Surface drag

For the drag of that part of the surface beneath the irrotational core, we take a conventional "power law" skin friction relation.
Equations (6.17, 12) and (6.17, 13) of Duncan, Thom and Young[8] give:

$$\left.\begin{aligned} C_f &\propto R_x^{-1/6} \\ \text{and} \quad \frac{C_F}{C_f} &= \frac{6}{5} \end{aligned}\right\} \tag{19}$$

where C_f and C_F are the respective local and average values of the skin-friction coefficient.

From equations (19) it follows that:

$$\text{Drag per unit span of region beneath irrotational core} = \frac{6}{5}\tau_c x_c \quad . \tag{20}$$

If the length of the entire surface is L, our reference drag is that of this surface entirely submerged in a uniform flow with the properties which the jet had initially, i.e.

$$\text{Reference drag} = \frac{6}{5}\tau_L L = \frac{6}{5}\tau_o L\left(\frac{x_o}{L}\right)^{1/6} \quad . \qquad (21)$$

Now, from equation (9), we have

$$\text{Drag per unit span beneath fully-developed wall-jet} = \tau_o \int_{x_o}^{L} \left(\frac{u_m}{u_j}\right)^{\beta} dx \quad . \qquad \ldots \quad (22)$$

The distribution of u_m/u_j is obtained from equation (13), with the virtual origin of the wall-jet flow given by equations (17) and (18). The exponent β, given by equation (10), has been determined from the work of R.P. Patel[3]. He found α to be approximately 1/6 and fitted a one-eleventh power law to his inner-layer velocity profiles. The resulting values of H and β are 1.18 and 2.36 respectively.

Equation (22) has been integrated on a computer for a range of L/h and u_j/u_e. The drag of the irrotational core region (equation (20)) has been added, and the total divided by the reference drag (equation (21)). In Fig.4 this quotient is plotted against L/h for a series of values of u_j/u_e.

4 APPLICATION TO THE ENGINE PROBLEM

4.1 Axial symmetry

The preceding analysis has been confined to planar flows. Since it is also confined to flows at constant pressure, its extension to treat axi-symmetric flows is effectively restricted to the case of cylindrical afterbodies. Thus radial convergence or divergence terms do not enter the analysis, and it may be used as it stands provided the afterbody diameter is large compared with the thickness y_m of the inner layer. In all cases of practical interest this will be so.

4.2 Compressibility

The application of the analysis to compressible flows requires further speculation. There is some evidence[9,10,11,12] that the spatial distribution

of velocity within turbulent boundary layers and shear layers is much less affected by compressibility than the use of a compressibility transformation (e.g. Ref.13) would suggest. Accordingly, by expressing quantities such as mixing rates as functions of the spatial velocity distribution, the effects of compressibility are substantially reduced if not eliminated.

On this basis we might suggest that the compressible problem, provided it is stated in terms of its geometry L/h and the jet/free stream velocity ratio u_j/u_e, reduces to an incompressible problem to which the results of section 2 may be applied unchanged.

One worthwhile simplification is however possible. Because of the work input by the fan, the total temperatures of jet and free stream are different. But, since the static pressures of jet and free stream are equal, and since the fan process is nearly isentropic, the static temperatures of jet and free stream are very nearly equal. Thus

$$\frac{u_j}{u_e} \simeq \frac{M_j}{M_e} \quad . \tag{23}$$

It is suggested therefore that Mach number ratio, which is readily evaluated from the fan pressure-ratio, be taken as the equivalent to the incompressible velocity ratio u_j/u_e in Fig.4.

4.3 Under-expanded jets

Strictly speaking, under-expanded jets, involving as they do pressure gradients downstream of the jet exit, are beyond the scope of the analysis. However, for large values of L/h these pressure gradients may not have an important effect on the total afterbody drag. If the analysis were to be applied to such jets, one important point should be noted: The orifice height h is not the actual height at the jet exit, but the height that would be necessary to pass the fan mass-flow if it were correctly expanded to free stream static pressure*. Similarly M_j is the Mach number the jet flow would attain when fully expanded.

---

*We might expect some alteration to equation (16) to be necessary. However, the rates of growth of the boundary layer and free shear layer are probably only weakly influenced by the expansion process and there seems no simple way of allowing for this influence. Since this particular application of the analysis becomes increasingly approximate as L/h diminishes, the further approximation of using equation (16) as it stands is thought to be unimportant.

4.4 Reference drag

Finally, for the particular case of a constant-pressure cylindrical afterbody, we may derive a simple approximate expression for its reference drag in terms of the properties of the free stream and the Mach number of the fan jet.

First we note that, since the static pressure in jet and free stream are equal,

$$\frac{q_j}{q_e} = \left(\frac{M_j}{M_e}\right)^2 \quad . \tag{24}$$

Also, as observed in section 4.2, the static temperatures of the two streams are very nearly equal; therefore their kinematic viscosities are also nearly equal and

$$\frac{\text{jet unit Reynolds number}}{\text{free-stream unit Reynolds number}} \simeq \frac{u_j}{u_e} \simeq \frac{M_j}{M_e} \quad . \tag{25}$$

To predict skin-friction coefficient we follow Appendix C of the paper by Sommer and Short[14]. The analysis is simplified by assuming that:

(i) viscosity is proportional to temperature;

(ii) skin-friction coefficient varies inversely as the one-sixth power of Reynolds number (equations (19));

(iii) recovery factor at the wall is 0.9.

If the skin-friction law for incompressible flow is written

$$C_F = CR^{-1/6} \quad , \tag{26}$$

it is readily shown from Sommer and Short that, for zero heat transfer,

$$\frac{\text{reference drag per unit span}}{\frac{1}{2}\rho_j u_j^2 L} = C_{Fj} = CR_j^{-1/6}\,(1 + 0.116\,M_j^2)^{-2/3} \quad . \tag{27}$$

Similarly, for a cylinder of the same length as the afterbody immersed in the free stream,

$$\frac{\text{drag per unit span in free stream}}{\frac{1}{2}\rho_\infty u_\infty^2 L} = C_{F\infty} = CR_\infty^{-1/6}\,(1 + 0.116\,M_\infty^2)^{-2/3} \quad . \qquad \ldots \quad (28)$$

Noting equations (24) and (25), and assuming that $M_e = M_\infty$, we now have

$$\frac{\text{reference drag per unit span}}{\frac{1}{2}\rho_\infty u_\infty^2 L} = C_{F\infty}\left(\frac{M_j}{M_\infty}\right)^{11/6}\left(\frac{1 + 0.116\,M_\infty^2}{1 + 0.116\,M_j^2}\right)^{2/3}$$

$$= C_{FR} \quad . \qquad (29)$$

In Fig.5 $C_{FR}/C_{F\infty}$ is plotted against M_j/M_∞ for three values of M_∞.

To predict afterbody drag, the average skin-friction coefficient $C_{F\infty}$ is determined from the Reynolds number of the afterbody at free stream conditions (in a manner consistent with the drag estimates for the rest of the aircraft), C_{FR} is then evaluated from equation (29) or Fig.5, and total friction coefficient, including wall-jet effects, finally estimated from Fig.4.

5 DISCUSSION

From Fig.5 it is apparent that the high-velocity stream from a front fan increases afterbody friction drag per unit wetted area appreciably. The main result of the present analysis, Fig.4, is that the alleviation of afterbody drag due to wall-jet effects will be small in most practical situations.

The analysis is essentially approximate. The major assumptions are:

(i) that equation (4) holds good for a wall-jet of moderate velocity ratio u_m/u_e;

(ii) that equation (13) adequately describes the decay of peak velocity of such a jet;

(iii) that the method of determining the virtual origin of the wall-jet (section 3.3) is realistic;

(iv) that the allowance for compressibility effects (section 4.2) is realistic.

A further important assumption, mentioned in section 2, is that the vorticity shed from the fan will have no significant effect on either the

mixing between jet and free stream or on the relationship between C_f and R_θ. This may well be in error, and an early experimental assessment of it would seem advisable.

To check the remaining assumptions would require a considerable experimental programme. In its absence, we may observe that in most practical cases wall-jet effects are likely to be small and the approximate nature of the wall-jet analysis therefore relatively unimportant.

Finally, attention is drawn to Appendix B in which the experimental work of Lawrence[5] is discussed. No firm explanation of the difference between these experiments and the present theory is offered, but reservations concerning the accuracy of the experiments are made. Accordingly, we suggest that until these differences are resolved the present theory offers the more reliable basis for performance estimates.

6 CONCLUSIONS

The drag of a two-dimensional turbulent wall-jet beneath a moving stream in incompressible flow at constant pressure has been analysed.

The results of this analysis are applied to the drag of a cylindrical afterbody immersed in the jet from a front fan with short cowl.

Graphs are presented which allow rapid evaluation of afterbody drag for a range of jet pressure ratios and nacelle geometries.

In most practical situations, the drag reduction over the afterbody due to mixing between the fan jet and free stream is likely to be small or non-existent.

Appendix A

THE MOMENTUM INTEGRAL EQUATION FOR THE WALL-JET INNER LAYER

Consider the flow between the wall and y_m, the locus of the velocity maximum. We may write the continuity and streamwise momentum equations respectively

$$\frac{d}{dx}\int_0^{y_m} u\,dy + v_m - u_m\frac{dy_m}{dx} = 0 \qquad \text{(A-1)}$$

and

$$\frac{d}{dx}\int_0^{y_m} u^2 dy + u_m\left(v_m - u_m\frac{dy_m}{dx}\right) + \frac{\tau_w}{\rho} - \frac{\tau_m}{\rho} = 0 \qquad \text{(A-2)}$$

whence, eliminating $v_m - u_m\frac{dy_m}{dx}$, we have

$$\frac{d}{dx}\int_0^{y_m} u^2 dy - u_m\frac{d}{dx}\int_0^{y_m} u\,dy + \frac{\tau_w}{\rho} - \frac{\tau_m}{\rho} = 0 \ . \qquad \text{(A-3)}$$

But θ is defined by

$$u_m^2\theta = u_m\int_0^{y_m} u\,dy - \int_0^{y_m} u^2 dy \qquad \text{(A-4)}$$

which yields on differentiation

$$u_m^2\frac{d\theta}{dx} + 2u_m\theta\frac{du_m}{dx} = \frac{du_m}{dx}\int_0^{y_m} u\,dy + u_m\frac{d}{dx}\int_0^{y_m} u\,dy - \frac{d}{dx}\int_0^{y_m} u^2 dy \ . \qquad \text{(A-5)}$$

Combining equations (A-3) and (A-5) we obtain

$$u_m^2\frac{d\theta}{dx} = \frac{\tau_w - \tau_m}{\rho} - 2u_m\theta\frac{du_m}{dx} + \frac{du_m}{dx}\int_0^{y_m} u\,dy \ . \qquad \text{(A-6)}$$

But

$$\int_0^{y_m} u \, dy = u_m (y_m - \delta^*) \quad . \tag{A-7}$$

Thus, finally, we have

$$\frac{d\theta}{dx} = \frac{\tau_w - \tau_m}{\rho u_m^2} + \frac{1}{u_m} \frac{du_m}{dx} [y_m - \delta^* - 2\theta] \quad . \tag{A-8}$$

Appendix B

EXPERIMENTS BY R.L. LAWRENCE

The most widely reported experimental study of this problem is by Lawrence[5]. He measured the friction drags of cylindrical afterbodies immersed in jets with Mach numbers (fully expanded) ranging from 1.05 to 1.62. Drag was obtained with the jets exhausting both into still air and into a Mach 0.8 stream. All jets were under-expanded, being sonic at their exit plane.

The divergence between Lawrence's experiments and the predictions of this Report are such that detailed comparisons are hardly justified. Firstly, scatter of the data is such that no firm test of the predicted variation of drag with L/h, Fig.4, is possible. Secondly, and more important, the observed variation of drag with jet Mach number differs significantly from that deduced from Fig.5.

This point is illustrated in Fig.6, where Lawrence's measured values of the friction coefficient C_{Fj} (equation (27)), for the case when the irrotational core of the jet extends beyond the afterbody, are plotted against jet pressure ratio. Also shown are values predicted by the method of Sommer and Short. C_{Fj} is effectively the drag coefficient of a flat plate, so for fully turbulent boundary layers we may expect these predictions, in particular their trend with pressure ratio, to be fairly reliable. The opposite trend shown by the data might therefore be taken as an indication of some anomalous feature in the experiments.

Lawrence himself notes the high drag in tests at high pressure ratio with some surprise. He suggests the high turbulence level in a wall jet, aggravated by a high initial turbulence level in his experiments due to turning the jet flow through 180° in its approach to the nozzle, as a possible explanation. However, the high turbulence in a fully developed wall-jet is irrelevant to C_{Fj}. Further, if the turbulence level of the initial jet flow was having an influence, we should expect it to affect the trend of overall drag C_{FT} with L/h (the experiments were performed by varying h and thus the contraction ratio of the orifice) but not the trend of C_{Fj} with pressure ratio (since the orifice was always choked, varying pressure ratio with h constant changed densities but not velocities in the supply pipe). The experimental trend of C_{FT} with L/h does not suggest that initial turbulence was an important factor.

Three other possible explanations are: a systematic error in drag measurement which was a function of jet pressure, appreciable movement of the transition position with varying jet pressure, or some effect of the flow acceleration from the sonic throat to its fully expanded state. The latter seems unlikely, since the region of flow adjustment was not particularly large, and in any case it is not obvious that the drag in the adjustment region should be greater than the drag over the same length of surface in a fully expanded flow. On the other hand, the trend of the data is qualitatively consistent with transition movement, even though both the absolute magnitudes of and the relative variations in C_{Fj} seem rather large to be explained in these terms. Reynolds number per foot varied between 6.5 and 13.5 million for jet pressure ratios between 2.0 and 4.4, and afterbody lengths were 0.5, 0.75 and 1.0 ft. Lawrence however gives no information on transition position.

The third of the above explanations, error in drag measurement, is also qualitatively consistent with the data. Moreover, precise measurements of friction drag using a balance become particularly difficult when, as seems to have been the case in Lawrence's experiments, appreciable pressure forces have to be allowed for.

A good check of this type of balance result could be provided by using surface pitot tubes to measure local wall shear-stress. At the same time a fair indication of the position of transition, and of the variation of wall shear-stress through the transition region, could be obtained. In any future experiments of this type, therefore, it would seem important not to miss the opportunity of obtaining an independent test of the balance results by means of this technique.

For the present, we must accept that the trend of C_{Fj} with pressure ratio observed by Lawrence could well be caused by transition movement or by a systematic error in drag measurement or both. In such circumstances it is difficult to feel confident that these results can be meaningfully extrapolated to aircraft scale. Accordingly their use in performance calculations is viewed with some reservation.

SYMBOLS

A, B, C	constants in skin-friction/Reynolds number relations, equations (1), (8) and (26)
C_f	local skin-friction coefficient
C_F	average skin-friction coefficient
C_{Fj}	equation (27)
$C_{F\infty}$	equation (28)
C_{FR}	equation (29)
C_{FT}	$\frac{2}{\rho_\infty u_\infty^2 L} \times$ total afterbody drag / afterbody circumference
F	rate of entrainment of jet core by free shear layer in the region $x < x_c$
h	initial height of fully expanded jet
H	inner-layer shape parameter ($= \delta^*/\theta$)
L	length of afterbody
M	Mach number
p	pressure
q	dynamic pressure $\frac{1}{2} \rho u^2$
R, R_x	length Reynolds number
R_θ	momentum thickness Reynolds number
u, v	components of velocity in x and y directions
x, y	co-ordinates respectively along and normal to surface
x'	streamwise co-ordinate with origin at virtual origin of wall-jet flow
α	exponent in skin-friction/Reynolds number relation, equation (1)
β	equation (10)
δ	boundary-layer thickness ($x < x_c$)
δ^*	inner-layer displacement thickness } equations (2)
θ	inner-layer momentum thickness } equations (2)
λ	jet "excess momentum thickness", equation (12)
ν	kinematic viscosity
ρ	density
τ	shear stress

SYMBOLS (Contd.)

Subscripts

c	denotes conditions at limit of irrotational core (Fig.1)
e	denotes properties of the external stream
j	denotes properties of the jet irrotational core
L	denotes conditions at downstream end of afterbody
m	denotes conditions at the velocity maximum in wall-jet flow ($x > x_c$)
o	denotes stagnation conditions
w	denotes conditions at the wall
∞	denotes free stream conditions

REFERENCES

No.	Author	Title, etc.
1	P. Bradshaw M.T. Gee	Turbulent wall jets with and without an external stream. A.R.C. R & M 3252 (A.R.C. 22008) (1960)
2	A. Sigalla	Measurements of skin friction in a plane turbulent wall jet. J. R.Ae.S., Vol.62, p.873 (1958)
3	R.P. Patel	Self-preserving, two-dimensional turbulent jets and wall jets in a moving stream. M. Eng. Thesis Dept of Mech Eng McGill University (1962)
4	W.H. Schwarz W.P. Cosart	The two-dimensional turbulent wall jet. J. Fluid Mech., Vol.10, p481 (1961)
5	R.L. Lawrence	Afterbody flow fields and skin friction on short duct fan nacelles. J. Aircraft, Vol.2, No.4, p318 (1965) (slightly revised version of AIAA paper 64-607)
6	L.J.S. Bradbury M.J. Riley	The spread of a turbulent plane jet issuing into a parallel moving airstream. J. Fluid Mech., Vol.27, p381 (1967)
7	J.E. Green	Two-dimensional turbulent reattachment as a boundary-layer problem. R.A.E. Technical Report 66059 (A.R.C. 28169) (1966)
8	W.J. Duncan A.S. Thom A.D. Young	The mechanics of fluids. Arnold (London) (1960)
9	J.M. Eggers	Velocity profiles and eddy viscosity distributions downstream of a Mach 2.22 nozzle exhausting to quiescent air. NASA TN D-3601
10	K.G. Winter K.G. Smith L. Gaudet	Unpublished Mintech Report (1965)

REFERENCES (Contd.)

No.	Author	Title, etc.
11	J.E. Green	The prediction of turbulent boundary layer development in compressible flow. J. Fluid Mech. Vol.31, Part 4, p.753 (1968)
12	G. Maise H. McDonald	Mixing length and kinematic eddy viscosity in a compressible boundary layer. AIAA Paper 67-199
13	A. Mager	Transformation of the compressible turbulent boundary layer. J. Aeronaut. Sci., Vol.25, p.305 (1958)
14	S.C. Sommer Barbara J. Short	Free flight measurements of turbulent boundary layer skin friction in the presence of severe aerodynamic heating at Mach numbers from 2.8 to 7.0. NACA TN 3391 (A.R.C. 17614) (1955)

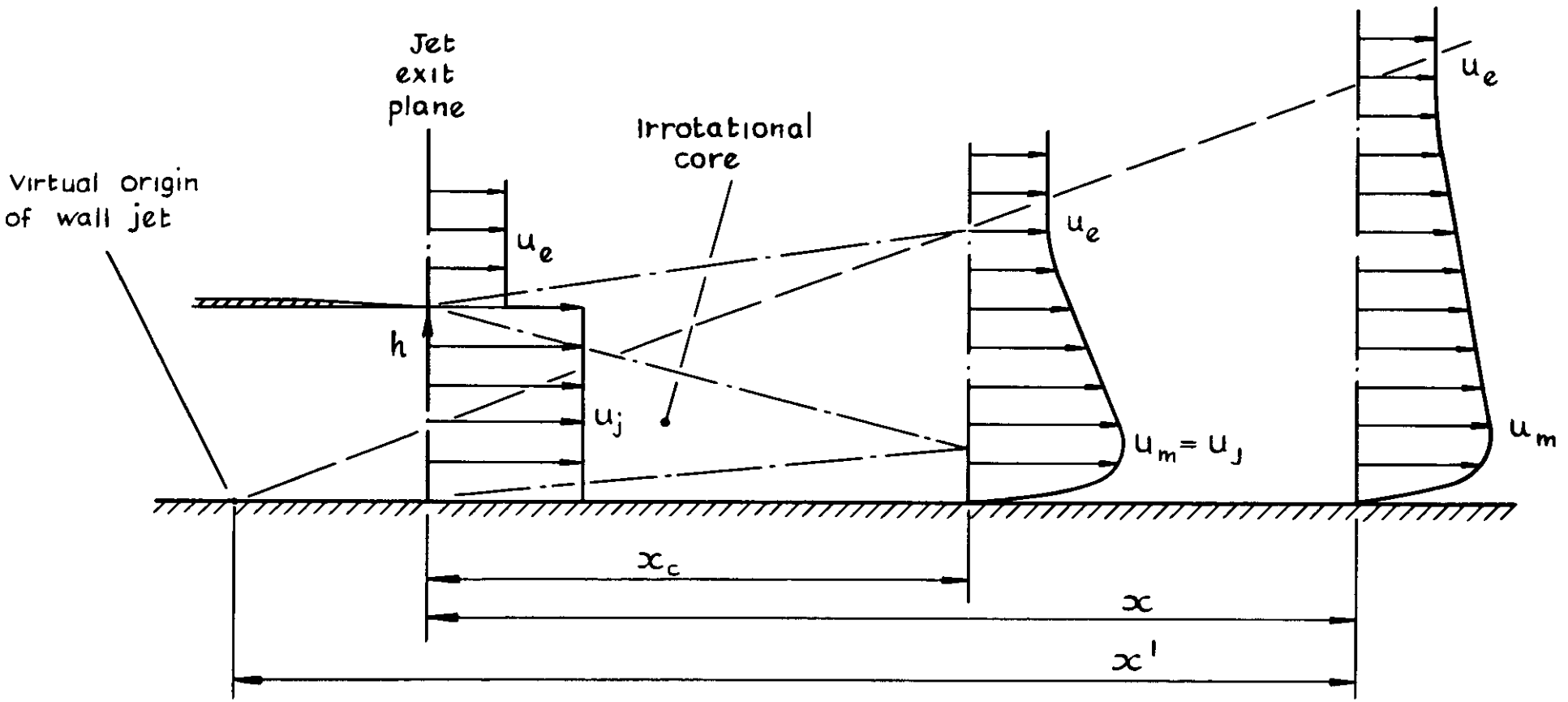

Fig 1 Two-dimensional jet beneath a moving stream (schematic)

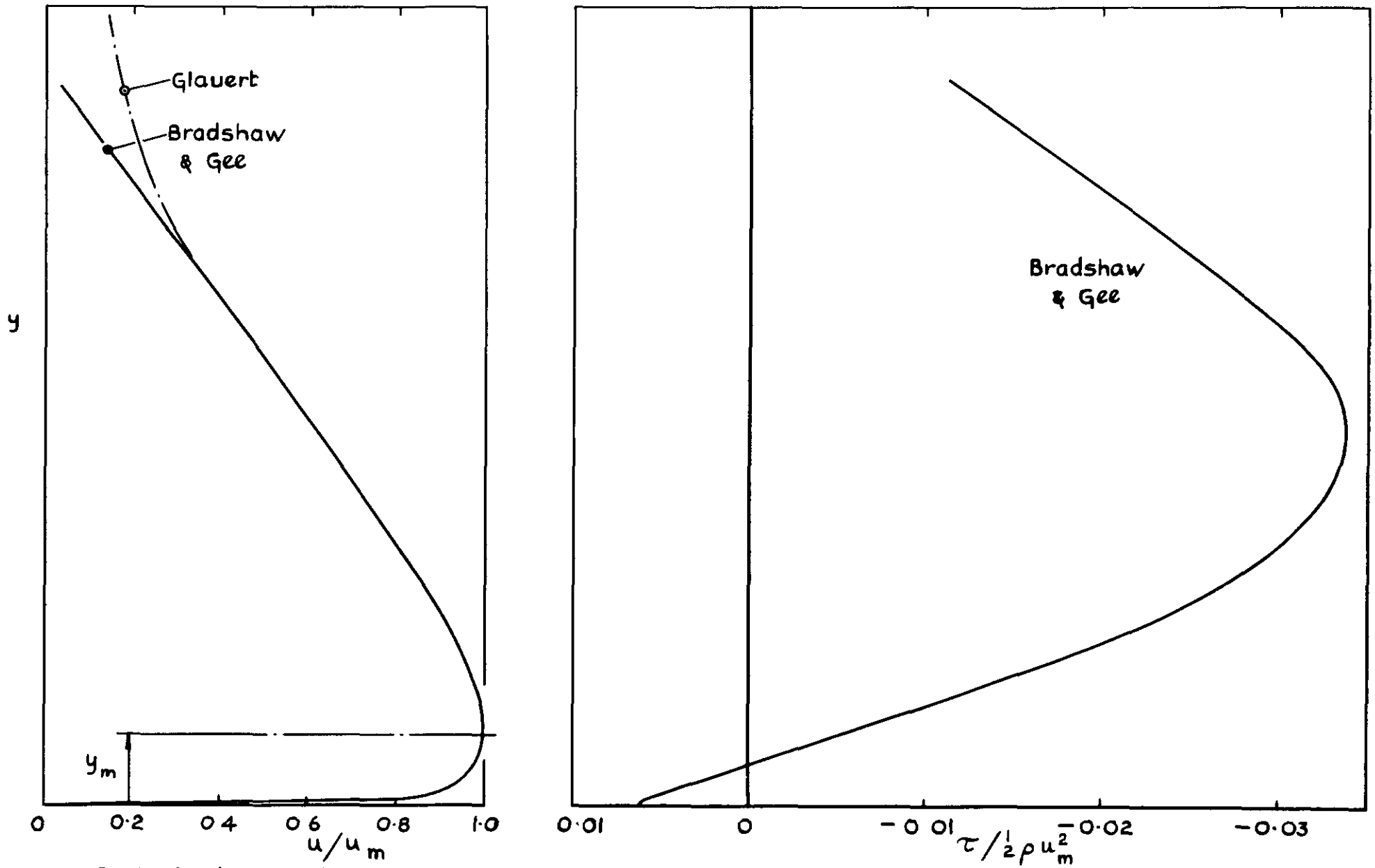

Fig 2 Velocity and shear-stress distributions for a wall jet flowing into still air

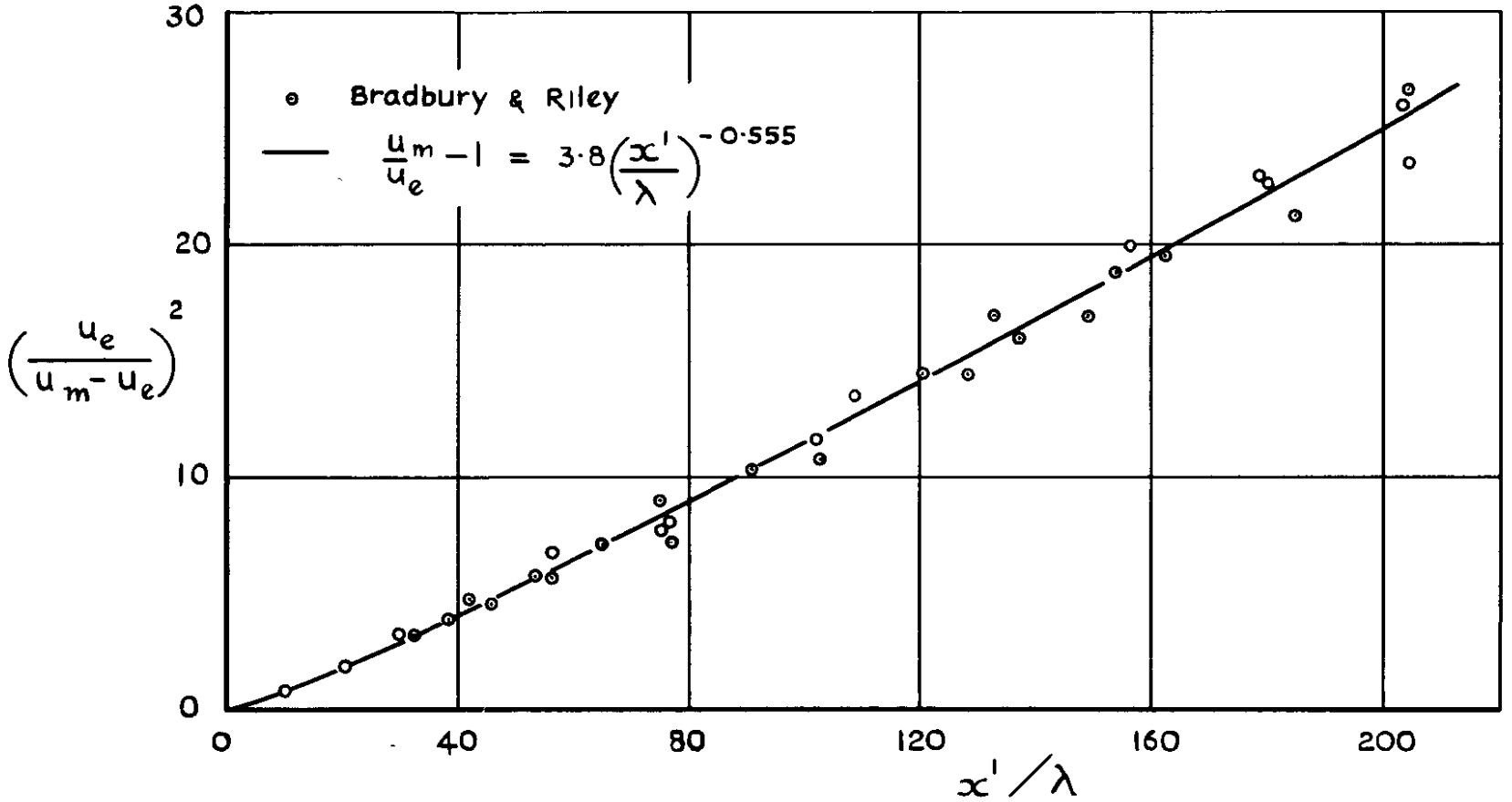

Fig. 3 Velocity delay along central plane of a free jet

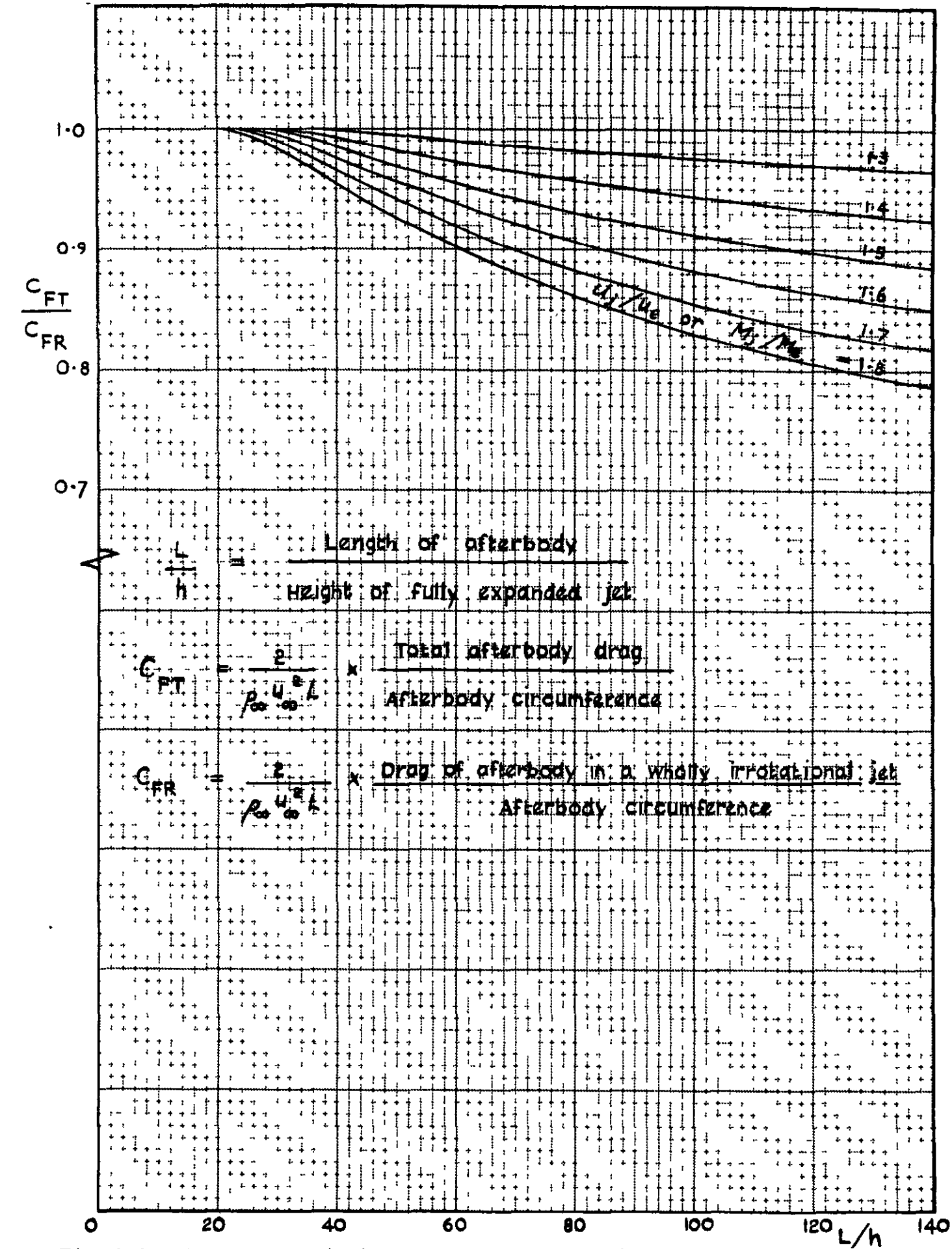

Fig.4 Ratio of total drag to reference drag as a function of L/h and jet Mach number ratio

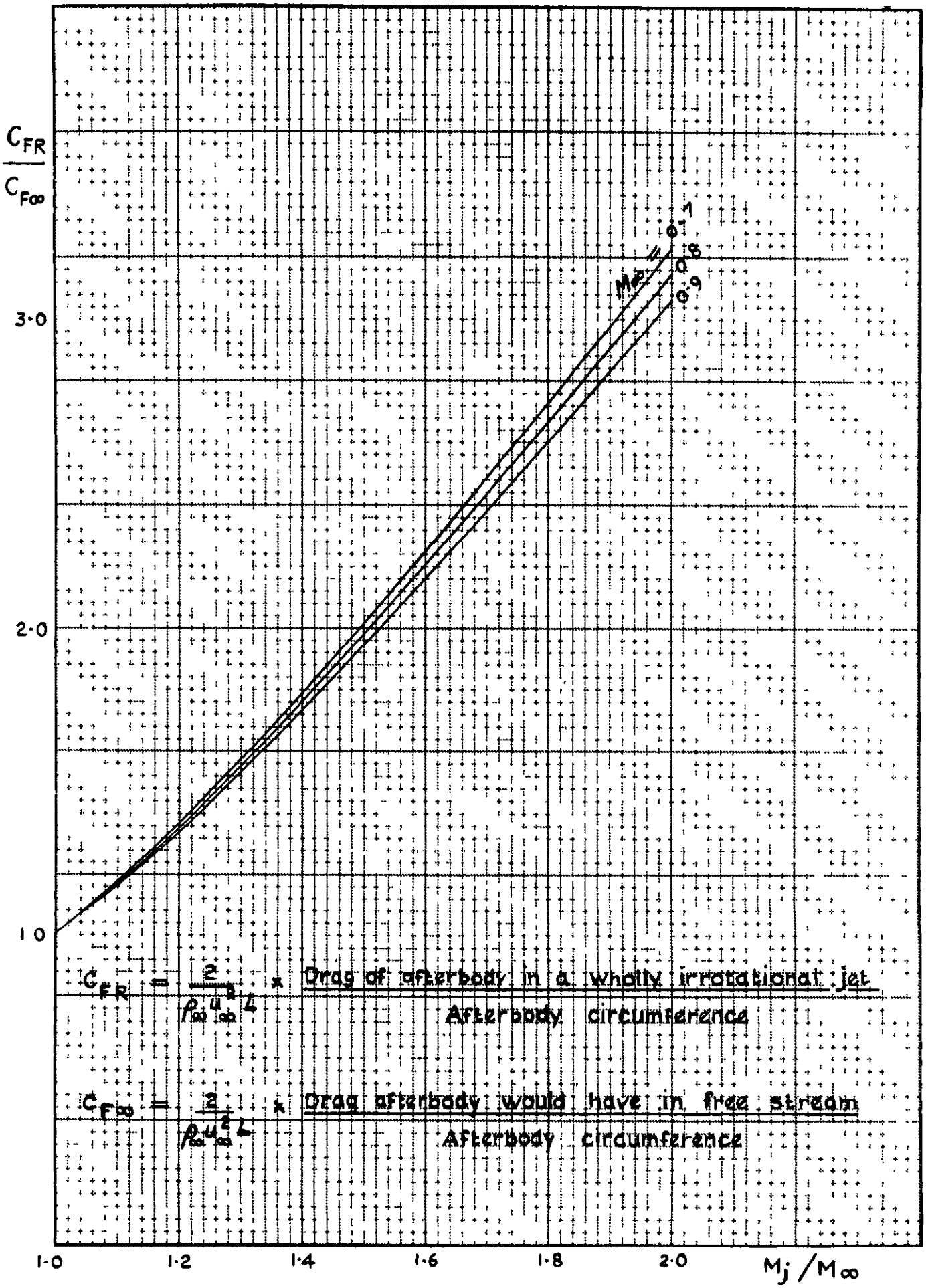

Fig.5 Variation of reference drag with jet Mach number ratio

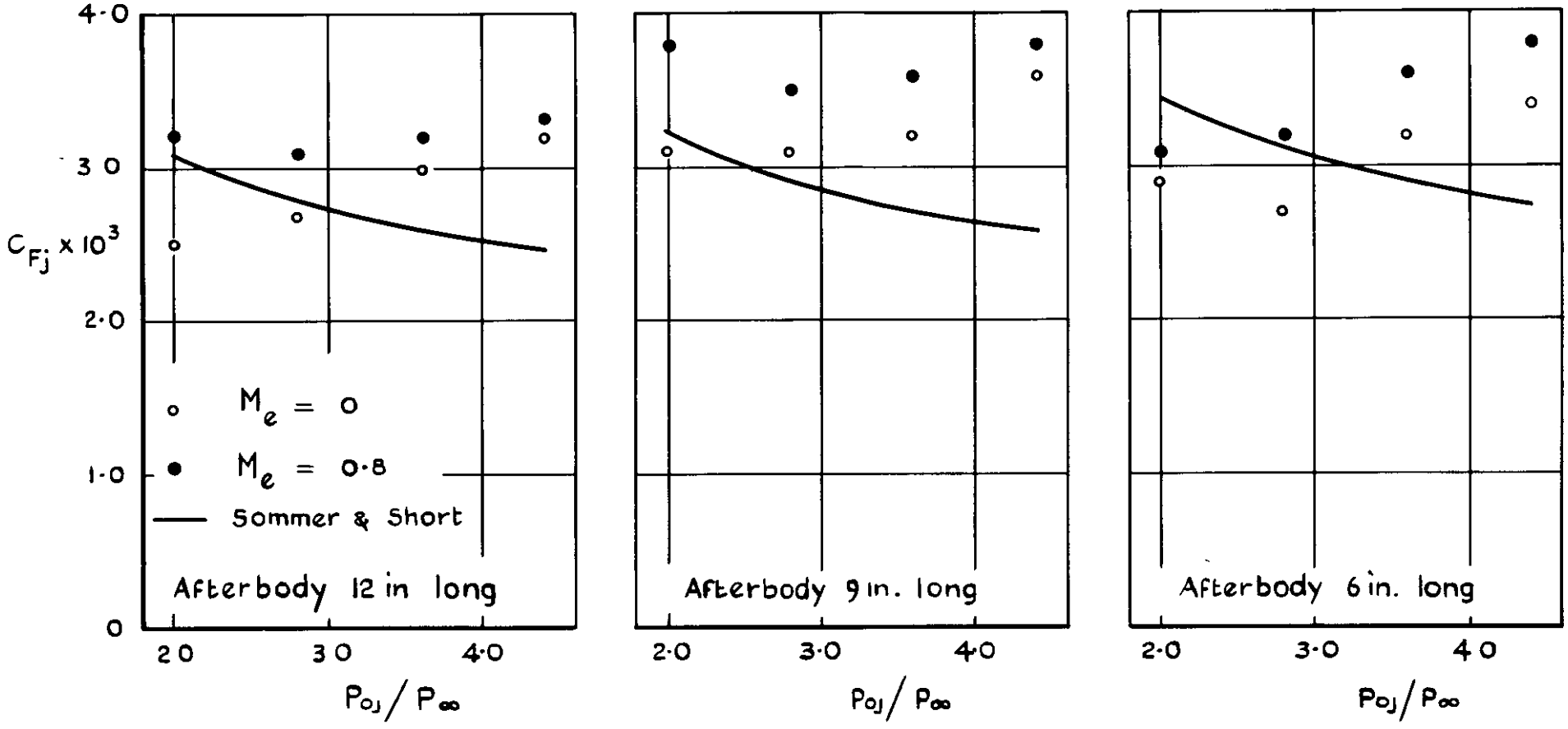

Fig.6 Drag measurements by Lawrence compared with those predicted by the method of Sommer and Short

Printed in England for Her Majesty's Stationery Office by the Royal Aircraft Establishment, Farnborough. Dd.146815. K.3.

A.R.C. C.P. No.1049
June 1967

Green, J.E.

621.438 + 629.13.038.5 :
533.6.013.124 :
629.13.012.122 :
533 697.4 :
533.695.27 :
533.696.8

SHORT-COWL FRONT-FAN TURBOJETS; FRICTION DRAG AND WALL-JET EFFECTS ON CYLINDRICAL AFTERBODIES

An approximate analysis is given of a turbulent wall-jet beneath a stream moving at constant velocity. The results of this analysis are used to predict the drag of a cylindrical afterbody immersed in the jet from a front fan with short cowl at subsonic flight speeds. Graphs are presented which allow rapid evaluation of afterbody drag for a range of jet pressure ratios and nacelle geometries.

A.R.C. C.P. No.1049
June 1967

Green, J.E.

621.438 + 629.13.038.5 :
533.6.013.124 :
629.13.012.122 :
533.697.4 :
533.695.27 :
533.696.8

SHORT-COWL FRONT-FAN TURBOJETS; FRICTION DRAG AND WALL-JET EFFECTS ON CYLINDRICAL AFTERBODIES

An approximate analysis is given of a turbulent wall-jet beneath a stream moving at constant velocity. The results of this analysis are used to predict the drag of a cylindrical afterbody immersed in the jet from a front fan with short cowl at subsonic flight speeds. Graphs are presented which allow rapid evaluation of afterbody drag for a range of jet pressure ratios and nacelle geometries.

A.R.C. C.P. No.1049
June 1967

Green, J.E.

621.438 + 629.13.038.5 :
533.6.013.124 :
629.13.012.122 :
533.697.4 :
533.695.27 :
533.696.8

SHORT-COWL FRONT-FAN TURBOJETS; FRICTION DRAG AND WALL-JET EFFECTS ON CYLINDRICAL AFTERBODIES

An approximate analysis is given of a turbulent wall-jet beneath a stream moving at constant velocity. The results of this analysis are used to predict the drag of a cylindrical afterbody immersed in the jet from a front fan with short cowl at subsonic flight speeds. Graphs are presented which allow rapid evaluation of afterbody drag for a range of jet pressure ratios and nacelle geometries.

A.R.C. C.P. No.1049
June 1967

Green, J.E.

621.438 + 629.13.038.5 :
533.6.013.124 :
629.13.012.122 :
533.697.4 :
533.695.27 :
533.696.8

SHORT-COWL FRONT-FAN TURBOJETS; FRICTION DRAG AND WALL-JET EFFECTS ON CYLINDRICAL AFTERBODIES

An approximate analysis is given of a turbulent wall-jet beneath a stream moving at constant velocity. The results of this analysis are used to predict the drag of a cylindrical afterbody immersed in the jet from a front fan with short cowl at subsonic flight speeds. Graphs are presented which allow rapid evaluation of afterbody drag for a range of jet pressure ratios and nacelle geometries.

DETACHABLE ABSTRACT CARDS

Published by
HER MAJESTY'S STATIONERY OFFICE

To be purchased from
49 High Holborn, London W C.1
13A Castle Street, Edinburgh 2
109 St. Mary Street, Cardiff CF1 1JW
Brazennose Street, Manchester 2
50 Fairfax Street, Bristol BS1 3DE
258 Broad Street, Birmingham 1
7 Linenhall Street, Belfast BT2 8AY
or through any bookseller

C.P. No. 1049

SBN 11 470176 8